


A *Caenorhabditis elegans* Male Pheromone Feminizes Germline Gene Expression in Hermaphrodites and Imposes Life-History Costs

David Angeles-Albores,[†] Erin Z. Aprison, Svetlana Dzitoyeva, and Ilya Ruvinsky ^{*}

Department of Molecular Biosciences, Northwestern University, Evanston, IL, USA

[†]Present address: Altos Labs, Bay Area Institute of Science, Redwood Shores, CA, USA

^{*}**Corresponding author:** E-mail: ilya.ruvinsky@northwestern.edu.

Associate editor: John True

Abstract

Sex pheromones not only improve the reproductive success of the recipients, but also impose costs, such as a reduced life span. The underlying mechanisms largely remain to be elucidated. Here, we show that even a brief exposure to physiological amounts of the dominant *Caenorhabditis elegans* male pheromone, *ascr#10*, alters the expression of thousands of genes in hermaphrodites. The most dramatic effect on the transcriptome is the upregulation of genes expressed during oogenesis and the downregulation of genes associated with male gametogenesis. This result reveals a way in which social signals help to resolve the inherent conflict between spermatogenesis and oogenesis in a simultaneous hermaphrodite, presumably to optimally align reproductive function with the presence of potential mating partners. We also found that exposure to *ascr#10* increased the risk of persistent intestinal infections in hermaphrodites due to pathological pharyngeal hypertrophy. Thus, our study reveals ways in which the male pheromone can not only have beneficial effects on the recipients' reproduction, but also cause harmful consequences that reduce life span.

Key words: pheromone, *C. elegans*, trade-off, transcriptome, germline, senescence.

Introduction

Sex pheromones alter multiple aspects of the recipient's reproductive biology (Wyatt 2014). We are studying these phenomena in a nematode *Caenorhabditis elegans*. In this species, hermaphrodites typically reproduce by selfing, but retain the ability to mate with males that are rare in both wild and laboratory populations (Frezal and Felix 2015). As is common in other species, "the *C. elegans* pheromone" is a complex blend of molecules (Srinivasan et al. 2008, 2012), including compounds that are predominantly produced by males (Ludewig et al. 2019; Burkhardt et al. 2023). The best-studied male pheromone, the ascaroside *ascr#10* (Izrayelit et al. 2012), at low physiological concentrations (Aprison and Ruvinsky 2017) modulates several reproduction-related traits in hermaphrodites in ways that appear to be beneficial. For example, it improves oocyte quality (Aprison et al. 2022) and increases the stores of germline precursors (Aprison and Ruvinsky 2016). On the other hand, *C. elegans* male pheromones generally (Maures et al. 2014; Booth et al. 2022) and *ascr#10* specifically (Aprison and Ruvinsky 2016; Ludewig et al. 2019) reduce the hermaphrodite life span.

The specific molecular mechanisms by which *ascr#10* alters hermaphrodite physiology remain largely unknown. It is reasonable to posit, however, that the reproductive

system is a major target of this pheromone. *Caenorhabditis elegans* is a simultaneous hermaphrodite. Morphologically, hermaphrodites resemble females, but they make a cache of sperm prior to irreversibly switching to oocyte production (Kimble and Crittenden 2007). Because hermaphrodites have reproductive organs of both sexes, they must balance resource investment between male and female functions that are inherently in conflict (Charnov 1979; Parker 2006). For males, the value of hermaphrodites resides in oocytes and other "female" traits, whereas hermaphrodite sperm and other "male" traits are a source of potential competition. We therefore hypothesized that one likely effect of the male pheromone is to bias hermaphrodites toward feminization at the expense of male functions (fig. 1a).

Results and Discussion

ascr#10 Feminizes the Hermaphrodite Transcriptome by Altering Expression of Thousands of Genes

Because altered gene expression likely undergirds the physiological effects of the pheromone, we assessed the changes caused by *ascr#10* in the global transcriptional profile of hermaphrodites (Aprison et al. 2022). Pheromone exposures were brief and took place after the switch from spermatogenesis to oogenesis. We assayed

© The Author(s) 2023. Published by Oxford University Press on behalf of Society for Molecular Biology and Evolution.

This is an Open Access article distributed under the terms of the Creative Commons Attribution-NonCommercial License (<https://creativecommons.org/licenses/by-nc/4.0/>), which permits non-commercial re-use, distribution, and reproduction in any medium, provided the original work is properly cited. For commercial re-use, please contact journals.permissions@oup.com

Open Access

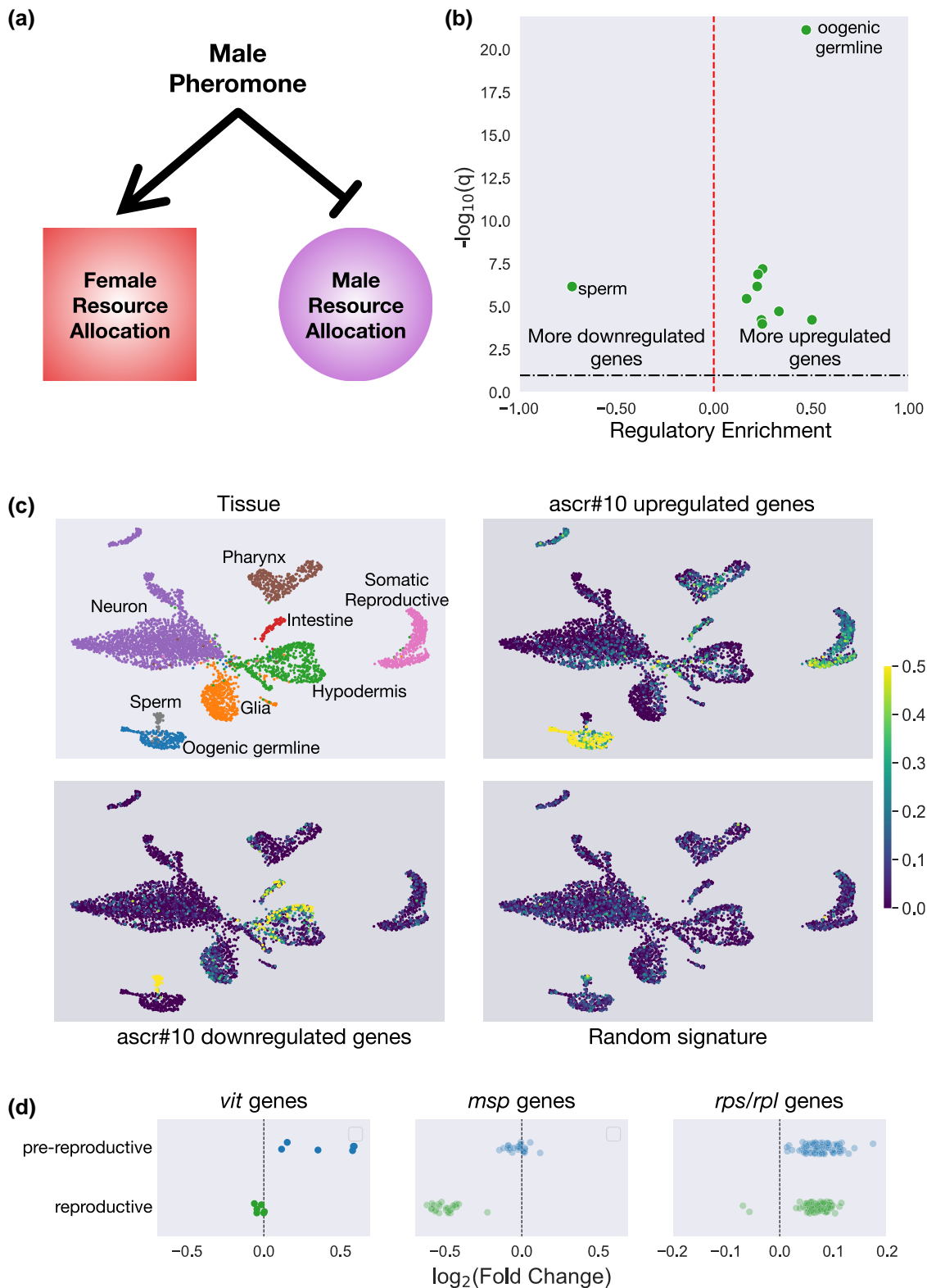


FIG. 1. Transcriptomic signature of shifting sex allocation in the presence of *ascr#10*. (a) The hypothesis tested in this study—exposure of hermaphrodites to the male pheromone is expected to increase allocation to “female” reproductive functions and decrease allocation to “male” reproductive functions. (b) Regulatory enrichment scores of tissues in response to *ascr#10* in reproductive animals. A positive regulatory enrichment score indicates that the fraction of genes that were differentially upregulated in response to *ascr#10* in that tissue is greater than expected by random chance. Only significantly enriched tissues are shown. (c) UMAP plot of single-cell RNA-seq data showing the tissue clusters. *ascr#10* upregulated genes are enriched in the oogenic germline, the somatic reproductive tissues, and the pharynx. Downregulated genes are expressed predominantly in hermaphroditic sperm, and the hypodermis. A random signature is shown for comparison. (d) Coherent differential expression of genes encoding vitellogenins (*vit*), Major Sperm Protein (*msp*), and ribosomal protein subunits (*rpl*, *rps*) implies that these groups of genes behave as functional units.

two timepoints—a few hours before and a few hours after the onset of egg-laying; we refer to these as prereproduction and reproduction, respectively.

We measured 12,244 genes across both timepoints. We identified 1,663 differentially expressed genes in prereproductive animals and 3,622 genes in reproductive animals in response to *ascr#10*. The magnitude of differential expression was modest (<2-fold for almost all genes), but changes were positively correlated across timepoints ([supplementary information, Supplementary Material](#) online). Aggregating weakly differentially expressed genes (those that show modest fold change) can be used to identify changes in organismal state ([Angeles-Albores et al. 2017](#)) or to reconstruct genetic pathways ([Angeles-Albores et al. 2018](#)).

Using previously curated WormBase annotations that assigned genes to tissues in which they are expressed, we evaluated whether differentially expressed genes were biased to specific cell types. Although upregulated genes were distributed across several tissues, the most notably overrepresented category was the oogenic germline, whereas the only downregulated tissue was sperm ([fig. 1b](#)).

A potential downside to this analysis is that it represents expression data as binary values (positive or negative) and relies on albeit expert, nonetheless human annotations. To overcome these limitations, we verified our results using a single-cell whole-organism RNA-seq data set ([Taylor et al. 2021](#)). We derived stringent signatures of genes up- or downregulated by *ascr#10* and computed expression-normalized scores per signature. We compared these scores to a random signature for reference. In broad agreement with the analysis based on curated annotations ([fig. 1b](#)), we saw that the *ascr#10* upregulated signature was enriched in the oogenic germline and the female reproductive soma, whereas the *ascr#10* downregulated signature was enriched among the sperm-expressed genes ([fig. 1c](#)).

Changes in expression in three functional classes of genes help to illustrate the response of the hermaphrodite transcriptome to *ascr#10* ([fig. 1d](#)). Yolk accounts for over one-third of total protein in the embryo, whereas vitellogenins that encode yolk proteins constitute approximately 3% of total adult mRNA ([Perez and Lehner 2019](#)). Expression of all vitellogenins was increased in prereproductive adults. The lack of enrichment in reproductive adults may be due to production being saturated. In reproductive adults, Major Sperm Protein (*msp*) genes ([Miller et al. 2001](#)) were downregulated. Finally, all genes encoding ribosomal proteins were upregulated, indicating increased demand for translational machinery. This result is consistent with the idea of greater offspring provision and the prior observation of increased ribosomal gene expression in mated hermaphrodites ([Booth et al. 2019](#)).

ascr#10 Increases Pharyngeal Pumping and Causes Pharyngeal Hypertrophy in Hermaphrodites

Because *ascr#10* increases expression of pharyngeal genes ([fig. 1b and c](#)), we quantified the effects of this male

pheromone on pharyngeal function and observed a significantly increased pumping rate ([fig. 2a](#)). We hypothesized that chronically increased pumping could lead to pharyngeal hypertrophy. Indeed, hermaphrodites raised in the presence of *ascr#10* had a significantly enlarged posterior bulb of the pharynx ([fig. 2b](#)). A similar swollen pharynx phenotype is a prevalent life span-limiting pathology identified in a necropsy analysis, with associated deaths proximally caused by bacterial infection ([Zhao et al. 2017](#)). Hermaphrodites aging in the presence of *ascr#10* showed considerably increased presence of live bacteria in the intestine ([fig. 2c](#)), suggesting that the pheromone-induced pharyngeal hypertrophy likely contributes to accelerated senescence.

Broad Effects of *ascr#10* on Reproduction-Related Traits and Longevity

There are six notable aspects of the response of *C. elegans* hermaphrodites to brief exposure to physiologically relevant ([Aprison and Ruvinsky 2017](#)) concentrations of the male pheromone *ascr#10*.

First, several thousand genes constituting over one-fourth of the detected genes showed significant change in expression, although nearly all by <2-fold. Therefore, the physiological and behavioral effects of *ascr#10* stem from modest fine-tuning of multiple genetic programs, not from substantial changes in a few select pathways. Broad changes in gene expression upon encountering the complete male pheromone bouquet were recently reported ([Booth et al. 2022](#)).

Second, the most conspicuous transcriptomic changes induced by *ascr#10* were the upregulation of the oogenic gene expression and the downregulation of the spermatogenic gene expression, demonstrating that a single component of the male pheromone is sufficient to feminize germline gene expression programs. Simultaneous hermaphrodites, such as *C. elegans*, must balance demands of sperm and oocyte production in the same organism ([Charnov 1979](#)). The male pheromone *ascr#10* signals to hermaphrodites the availability of male sperm and thus reduced need for self-sperm. We interpret the ensuing transcriptomic changes as tuning gene expression programs to optimize oogenesis, in line with the hypothesis in [figure 1a](#). We are not aware of an experimental demonstration of such a phenomenon in any species. Theory predicts that selection should favor deployment of reproductive resources by hermaphrodites (between male and female functions) which best reflects mating opportunities ([Charnov 1982](#)). Experimental evidence supports this idea. For example, hermaphrodites of the plant *Mercurialis annua* mating in the absence of males evolved greater male allocation ([Dorken and Pannell 2009](#)). Our results are consistent with feminization of the hermaphrodite germline transcriptome in the presence of a male pheromone.

Third, in our experiments, young adult hermaphrodites were exposed to the pheromone several hours after the

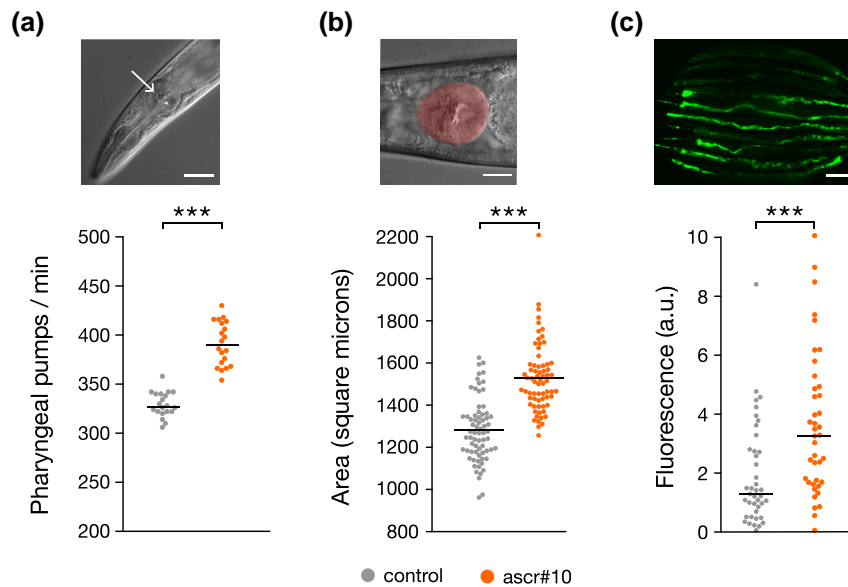


Fig. 2. The effects of *ascr#10* on pharyngeal function and morphology. (a) DIC image of the pharynx and rate of pharyngeal pumping in young adult hermaphrodites exposed to control or *ascr#10* for 1 h ($n = 20$). The arrow points to the grinder within the posterior bulb of the pharynx. Scale bar = 40 μm . (b) Area of the posterior bulb (highlighted by false coloring) in hermaphrodites (Day 8 of adulthood) raised on control or *ascr#10* ($n = 70$ for control and $n = 68$ for *ascr#10*). Scale bar = 20 μm . (c) Representative image and quantification of fluorescence in hermaphrodites (Day 8 of adulthood) raised on control or *ascr#10* and fed OP50 *Escherichia coli* expressing GFP ($n = 41$ for control and $n = 40$ for *ascr#10*). Scale bar = 200 μm . In all three panels, P -values are from Kolmogorov–Smirnov test; *** $P < 0.01$.

switch between spermatogenesis and oogenesis that occurs during the last larval stage (Kimble and Crittenden 2007). It may seem surprising that animals that are apparently irreversibly committed to oocyte production continue to express many genes associated with sperm production. Yet, transcriptome profiling of young adult hermaphrodites similar in age to the ones we used in this study shows substantial continued expression of genes associated with spermatogenesis (Ortiz et al. 2014; Ebbing et al. 2018). These results indicate that the binary switch in the type of produced gametes is undergirded by a more gradual change in gene expression. A switch from spermatogenesis to oogenesis is thought to involve the release of posttranscriptional repression of oogenic transcripts (Noble et al. 2016). Understanding how (or whether) this process is related to the male pheromone-induced bias of the pool of mRNAs toward oogenic profile may be instructive for understanding germline development in *C. elegans*. Our findings raise additional questions. Is the differential gene expression on *ascr#10* primarily due to transcriptional or posttranscriptional (Merritt et al. 2008) mechanisms? Do the changes in the oogenic gene expression induced by *ascr#10* result from an increase in the number of oocyte precursors or the alteration of mRNA profiles in a specific subset of these cells?

Fourth, *C. elegans* hermaphrodites continue to respond to male pheromones even though males and mating are relatively rare in natural populations (Frezal and Felix 2015). Why is this relic of the ancestral gonochoristic mode of reproduction (Cutter et al. 2019) retained in a hermaphroditic species? In natural habitats, worms commonly experience stress conditions that increase the

frequency of males. The resulting outcrossing is favored and advantageous under such conditions (Morran, Cappy et al. 2009; Morran, Parmenter et al. 2009). We propose that increased reproductive success conferred by *ascr#10* in challenging environments contributes to the retention of this male pheromone in a hermaphroditic species. Consistent with this idea, *ascr#10* facilitates reproductive recovery from heat stress (Aprison and Ruvinsky 2015).

Fifth, interactions with males are detrimental to *C. elegans* hermaphrodites (Shi and Murphy 2014; Ting et al. 2014; Booth et al. 2022) and some deleterious effects are due to male-excreted compounds (Maures et al. 2014; Shi et al. 2017). Previously, we showed that *ascr#10* shortens the hermaphrodite life span (Aprison and Ruvinsky 2016; Ludewig et al. 2019). The physiological changes induced by male pheromones that reduce longevity are only beginning to be understood. Our work has identified three plausibly detrimental effects of *ascr#10* that likely contribute to the shortening of the hermaphrodite life span. 1) Pharyngeal hypertrophy and the associated persistent bacterial infections (fig. 2). 2) Increased yolk production in hermaphrodites (fig. 1d) can result in senescent pathologies (Garigan et al. 2002; Zimmerman et al. 2015; Seah et al. 2016; Ezcurra et al. 2018), mutations that promote longevity decrease vitellogenin expression (DePina et al. 2011), reduction of vitellogenin expression increases life span (Murphy et al. 2003) and, in general, yolk production has opposite effects on reproductive success and longevity (Wu et al. 2022). Mating, which includes exposure to male pheromones, promotes vitellogenesis (DePina et al. 2011). 3) Physiological cell death in the

germline is increased by *ascr#10* and is required for improving oocyte quality (Aprison et al. 2022), but it may result in gonad pathologies (de la Guardia et al. 2016). There are possibly other ways in which *ascr#10* reduces hermaphrodite longevity. For this reason and because *ascr#10* is the only one of many pheromone components produced by *C. elegans* males (Burkhardt et al. 2023), several of which could reduce hermaphrodite life span, for example (Ludewig et al. 2019), multiple pathways likely contribute to accelerated senescence in response to male signals. The currently available evidence is consistent with this idea (Maures et al. 2014; Shi and Murphy 2014; Booth et al. 2022).

Finally, “why” do male pheromones cause earlier death in hermaphrodites? Because increased mortality starts soon after peak fertility, one possibility is that the males use pheromones to reduce competition for resources from postreproductive hermaphrodites or to prevent hermaphrodites’ mating with other males (Maures et al. 2014; Shi and Murphy 2014). The discovery that males are more susceptible to pheromone killing than hermaphrodites (Shi et al. 2017) and theoretical considerations (Cutter et al. 2019) suggest that hermaphrodite harm may not be the primary objective. Organisms operate under the constraints of a web of trade-offs between reproduction and soma maintenance (Maklakov and Chapman 2019) and increased investment in the “expensive germline” (Maklakov and Immler 2016) may necessarily compromise longevity. Viewed in this way, and consistent with the results presented here, the male pheromone promotes investment in the oogenic germline in youthful hermaphrodites at the cost of “collateral harm” (Parker 2006) of accelerated postreproductive senescence.

Materials and Methods

Analysis of Differential Gene Expression in Presence of *ascr#10*

We used the data from Aprison et al. (2022) to carry out all analyses (GSE193636). Briefly, wild-type N2 hermaphrodites were synchronized and exposed to *ascr#10* approximately 3–4 h after the L4-to-adult molt (48 h post release from L1 arrest). Germline production switches from spermatogenesis to oogenesis during the L4 stage (Kimble and Crittenden 2007). Worms were harvested for RNA preparation either approximately 3–4 h before the onset of reproduction (50 h post release from L1 arrest) or approximately 3–4 h after the onset of egg laying (58 h post release from L1 arrest).

We restricted analyses only to those genes that were identified across both conditions. Consequently, the number of differentially expressed genes in our analyses is smaller than previously reported (1,667 and 3,627 reported originally in prereproductive and reproductive animals in response to *ascr#10* vs. 1,663 and 3,622 reported here), but the fold changes and *q*-values are identical with Aprison et al. (2022).

All codes required to completely reproduce our analyses are available in GitHub (<https://github.com/dangeles/Ascr10xomics>). Statistical functions and large pieces of code were written as python v.3.7 (van Rossum and Drake 2009) scripts that can be loaded locally; the analyses are carried out in annotated Jupyter notebooks (Granger and Pérez 2021) which were used to generate the supplementary information, Supplementary Material online.

We tested tissues for directional enrichment using a binomial test. We downloaded the complete tissue expression annotations from WormBase (Davis et al. 2022). We restricted our analysis to tissues that had at least five annotated genes. We did not use genes if they had promiscuous tissue expression—we dropped any genes that were annotated in 30 or more terms. If a term had annotated genes that were all considered promiscuous, that term was also dropped. We tested terms for regulatory enrichment by using a binomial test, where the proportion of genes expected to increase expression was given by the net fraction of genes that were upregulated in each condition, followed by a Benjamini–Hochberg correction. Exclusively for visualization purposes, we removed redundant tissue terms by identifying terms that were >75% similar by Jaccard similarity and removing the term with fewer annotated gene expression levels. Tissues were concordant between the two compared timepoints (50 and 58 h post release from the L1 arrest), though *q*-values were lower postonset of reproduction.

For our analyses of the single-cell gene expression atlas (Taylor et al. 2021) using SCANPY (Wolf et al. 2018), we removed all cells annotated “Unknown” and “Unannotated.” We also removed “Muscle_mesoderm” cells because they clustered apart from the remaining cell types and distorted the uniform manifold approximation and projection (UMAP) diagrams; however, removing these cells did not alter our conclusions. We filtered cells that showed expression of fewer than 150 genes and removed any genes expressed in fewer than 50 cells. We removed cells that had fewer than 250 total counts, mitochondrial content <1% or >10%, riboprotein content <1% or >20%, and NADH enzyme content <0.3% or >3%. If a cell was annotated as a neuron, we removed cells that had <800 total counts, because we observed that neurons had much greater read content than the other cell types. Given the low read content, we normalized counts in cells to counts per thousand, as suggested previously (Lun 2018).

To generate UMAPs, we subsampled the data set to equally represent all tissues with 2,000 cells (or less if fewer cells were annotated in the data set). This allowed the UMAP to show better separation among tissues. We reduced the dimensionality of the data set using principal component analysis (PCA) and keeping the first 15 principal components. Next, we computed the 100 nearest neighbors per cell, and computed the UMAP using SCANPY’s UMAP function, initializing the UMAP with precomputed PAGA positions (Wolf et al. 2019). Next, we computed signature enrichment scores. To generate an *ascr#10*-upregulated (or downregulated) signature, we identified the genes that

were differentially expressed at 50 and 58 h (on vs. off ascr#10), that changed expression in the same direction, and that increased (decreased) expression in response to ascr#10. For comparison, we also generated a signature with 159 randomly selected genes. We calculated an enrichment score using SCANPY's "score_genes" function. This function reproduces the score derived in Satija et al. (2015), which works by computing the average expression level of the input signature genes and subtracting a random reference set of genes. The random reference set is chosen so that the distribution of average gene expression levels between the input and reference sets is similar.

Measurements of Pharyngeal Phenotypes in Hermaphrodites Exposed to ascr#10

Concentrated ascr#10 was stored in ethanol at -20°C . This stock was diluted with water and a total of 100 μl of ascaroside solution containing 2.2 femtograms per plate was applied to the plate and spread evenly with a sterile bent glass rod. Plates were incubated at 20°C overnight to allow the ascaroside to be absorbed. Control plates were prepared in the same manner using water as the control. The following day, the plates were seeded with 20 μl of a 1:10 dilution of OP50 overnight culture and allowed to grow overnight at 20°C before use. All experiments were conducted using wild-type N2 hermaphrodites.

To measure pharyngeal pumping rates, hermaphrodites were synchronized by hypochlorite treatment and tested at approximately 70 h post release from L1 arrest (Day 2 adults). Ten hermaphrodites per plate were transferred to either control plates or ascr#10 plates prepared as above and allowed to acclimate for 1 h. The number of pharyngeal pumps was counted for 20 s. This was done 3 \times for each worm waiting at least 20 s between counts.

To measure the area of the terminal bulb of the pharynx in worms that had been raised on control plates or ascr#10 plates, Day 8 adults were mounted on 2% agarose pads and images were recorded using a Leica DM5000B microscope fitted with a Retiga 2000R camera and quantified using ImageJ.

To measure intestinal colonization by bacteria, hermaphrodites were grown on either control or ascr#10 plates seeded with OP50 *Escherichia coli* carrying the pFPV25.1 plasmid that encodes green fluorescent protein (GFP). Worms were transferred every other day until they were Day 8 adults. Day 8 adults were mounted on 2% agarose pads and the slides were imaged on a Leica DM5000B microscope using a Retiga 2000R camera. Images were stitched together using the ImageJ plug-in (Preibisch et al. 2009). The entire intestine was outlined in each hermaphrodite and the corrected total fluorescence for each organ was determined in ImageJ. Since Day 8 adults exhibit increased autofluorescence (Teuscher and Ewald 2018), Day 8 adults raised on control or ascr#10 plates seeded with regular OP50 were also compared and the amount of autofluorescence was quantified as above.

Supplementary Material

Supplementary data are available at *Molecular Biology and Evolution* online.

Acknowledgments

The authors thank R. Morimoto for generous hospitality and F. Schroeder for ascr#10. This work was funded in part by the NIH (R01GM126125) grant to I.R. The authors also thank WormBase and the Caenorhabditis Genetics Center (CGC). WormBase is supported by grant U41 HG002223 from the National Human Genome Research Institute at the NIH, the UK Medical Research Council, and the UK Biotechnology and Biological Sciences Research Council. The CGC is funded by the NIH Office of Research Infrastructure Programs (P40 OD010440).

References

- Angeles-Albores D, Leighton DHW, Tsou T, Khaw TH, Antoshechkin I, Sternberg PW. 2017. The *Caenorhabditis elegans* female-like state: decoupling the transcriptomic effects of aging and sperm status. *G3 (Bethesda)* **7**:2969–2977.
- Angeles-Albores D, Puckett Robinson C, Williams BA, Wold BJ, Sternberg PW. 2018. Reconstructing a metazoan genetic pathway with transcriptome-wide epistasis measurements. *Proc Natl Acad Sci U S A.* **115**:E2930–E2939.
- Aprison EZ, Dzitoyeva S, Angeles-Albores D, Ruvinsky I. 2022. A male pheromone that improves the quality of the oogenic germline. *Proc Natl Acad Sci U S A.* **119**:e2015576119.
- Aprison EZ, Ruvinsky I. 2015. Sex pheromones of *C. elegans* males prime the female reproductive system and ameliorate the effects of heat stress. *PLoS Genet.* **11**:e1005729.
- Aprison EZ, Ruvinsky I. 2016. Sexually antagonistic male signals manipulate germline and soma of *C. elegans* hermaphrodites. *Curr Biol.* **26**:2827–2833.
- Aprison EZ, Ruvinsky I. 2017. Counteracting ascarosides act through distinct neurons to determine the sexual identity of *C. elegans* pheromones. *Curr Biol.* **27**:2589–2599.e3.
- Booth LN, Maures TJ, Yeo RW, Tantilert C, Brunet A. 2019. Self-sperm induce resistance to the detrimental effects of sexual encounters with males in hermaphroditic nematodes. *eLife* **8**:e46418.
- Booth LN, Shi C, Tantilert C, Yeo RW, Miklas JW, Hebestreit K, Hollenhorst CN, Maures TJ, Buckley MT, Murphy CT, et al. 2022. Males induce premature demise of the opposite sex by multifaceted strategies. *Nat Aging.* **2**:809–823.
- Burkhardt RN, Artyukhin AB, Aprison EZ, Curtis BJ, Fox BW, Ludwig AH, Palomino DF, Luo J, Chaturbedi A, Panda O, et al. 2023. Sex-specificity of the *C. elegans* metabolome. *Nat Commun.* **14**:320.
- Charnov EL. 1979. Simultaneous hermaphroditism and sexual selection. *Proc Natl Acad Sci U S A.* **76**:2480–2484.
- Charnov EL. 1982. *The theory of sex allocation*. Princeton (NJ): Princeton University Press.
- Cutter AD, Morran LT, Phillips PC. 2019. Males, outcrossing, and sexual selection in *Caenorhabditis* nematodes. *Genetics* **213**:27–57.
- Davis P, Zarowiecki M, Arnaboldi V, Becerra A, Cain S, Chan J, Chen WJ, Cho J, da Veiga Beltrame E, Diamantakis S, et al. 2022. WormBase in 2022—data, processes, and tools for analyzing *Caenorhabditis elegans*. *Genetics* **220**:iyac003.
- de la Guardia Y, Gilliat AF, Hellberg J, Rennert P, Cabreiro F, Gems D. 2016. Run-on of germline apoptosis promotes gonad senescence in *C. elegans*. *Oncotarget* **7**:39082–39096.
- DePina AS, Iser WB, Park SS, Maudsley S, Wilson MA, Wolkow CA. 2011. Regulation of *Caenorhabditis elegans* vitellogenesis by

- DAF-2/11S through separable transcriptional and posttranscriptional mechanisms. *BMC Physiol.* **11**:11.
- Dorken ME, Pannell JR. 2009. Hermaphroditic sex allocation evolves when mating opportunities change. *Curr Biol.* **19**:514–517.
- Ebbing A, Vertesy A, Betist MC, Spanjaard B, Junker JP, Berezikov E, van Oudenaarden A, Korswagen HC. 2018. Spatial transcriptomics of *C. elegans* males and hermaphrodites identifies sex-specific differences in gene expression patterns. *Dev Cell.* **47**:801–813.e6.
- Ezcurra M, Benedetto A, Sornda T, Gilliat AF, Au C, Zhang Q, van Schelt S, Petrache AL, Wang H, de la Guardia Y, et al. 2018. *C. elegans* eats its own intestine to make yolk leading to multiple senescent pathologies. *Curr Biol.* **28**:2544–2556.e5.
- Frezal L, Felix MA. 2015. *C. elegans* outside the Petri dish. *eLife* **4**:e05849.
- Garigan D, Hsu AL, Fraser AG, Kamath RS, Ahringer J, Kenyon C. 2002. Genetic analysis of tissue aging in *Caenorhabditis elegans*: a role for heat-shock factor and bacterial proliferation. *Genetics* **161**:1101–1112.
- Granger BE, Pérez F. 2021. Jupyter: thinking and storytelling with code and data. *Comput Sci Eng.* **23**:7–14.
- Izrayelit Y, Srinivasan J, Campbell SL, Jo Y, von Reuss SH, Genoff MC, Sternberg PW, Schroeder FC. 2012. Targeted metabolomics reveals a male pheromone and sex-specific ascarioside biosynthesis in *Caenorhabditis elegans*. *ACS Chem Biol.* **7**:1321–1325.
- Kimble J, Crittenden SL. 2007. Controls of germline stem cells, entry into meiosis, and the sperm/oocyte decision in *Caenorhabditis elegans*. *Annu Rev Cell Dev Biol.* **23**:405–433.
- Ludewig AH, Artyukhin AB, Aprison EZ, Rodrigues PR, Pulido DC, Burkhardt RN, Panda O, Zhang YK, Gudibanda P, Ruvinsky I, et al. 2019. An excreted small molecule promotes *C. elegans* reproductive development and aging. *Nat Chem Biol.* **15**:838–845.
- Lun A. 2018. Overcoming systematic errors caused by log-transformation of normalized single-cell RNA sequencing data. bioRxiv 404962. <https://doi.org/10.1101/404962>
- Maklakov AA, Chapman T. 2019. Evolution of ageing as a tangle of trade-offs: energy versus function. *Proc Biol Sci.* **286**:20191604.
- Maklakov AA, Immler S. 2016. The expensive germline and the evolution of ageing. *Curr Biol.* **26**:R577–R586.
- Maures TJ, Booth LN, Benayoun BA, Izrayelit Y, Schroeder FC, Brunet A. 2014. Males shorten the life span of *C. elegans* hermaphrodites via secreted compounds. *Science* **343**:541–544.
- Merritt C, Rasoloson D, Ko D, Seydoux G. 2008. 3' UTRs are the primary regulators of gene expression in the *C. elegans* germline. *Curr Biol.* **18**:1476–1482.
- Miller MA, Nguyen VQ, Lee MH, Kosinski M, Schedl T, Caprioli RM, Greenstein D. 2001. A sperm cytoskeletal protein that signals oocyte meiotic maturation and ovulation. *Science* **291**:2144–2147.
- Morran LT, Cappy BJ, Anderson JL, Phillips PC. 2009. Sexual partners for the stressed: facultative outcrossing in the self-fertilizing nematode *Caenorhabditis elegans*. *Evolution* **63**:1473–1482.
- Morran LT, Parmenter MD, Phillips PC. 2009. Mutation load and rapid adaptation favour outcrossing over self-fertilization. *Nature* **462**:350–352.
- Murphy CT, McCarroll SA, Bargmann CI, Fraser A, Kamath RS, Ahringer J, Li H, Kenyon C. 2003. Genes that act downstream of DAF-16 to influence the lifespan of *Caenorhabditis elegans*. *Nature* **424**:277–283.
- Noble DC, Aoki ST, Ortiz MA, Kim KW, Verheyden JM, Kimble J. 2016. Genomic analyses of sperm fate regulator targets reveal a common set of oogenic mRNAs in *Caenorhabditis elegans*. *Genetics* **202**:221–234.
- Ortiz MA, Noble D, Sorokin EP, Kimble J. 2014. A new dataset of spermatogenic vs. oogenic transcriptomes in the nematode *Caenorhabditis elegans*. *G3 (Bethesda)* **4**:1765–1772.
- Parker GA. 2006. Sexual conflict over mating and fertilization: an overview. *Philos Trans R Soc Lond B Biol Sci.* **361**:235–259.
- Perez MF, Lehner B. 2019. Vitellogenins - yolk gene function and regulation in *Caenorhabditis elegans*. *Front Physiol.* **10**:1067.
- Preibisch S, Saalfeld S, Tomancak P. 2009. Globally optimal stitching of tiled 3D microscopic image acquisitions. *Bioinformatics* **25**:1463–1465.
- Satija R, Farrell JA, Gennert D, Schier AF, Regev A. 2015. Spatial reconstruction of single-cell gene expression data. *Nat Biotechnol.* **33**:495–502.
- Seah NE, de Magalhaes Filho CD, Petrashen AP, Henderson HR, Laguer J, Gonzalez J, Dillin A, Hansen M, Lapierre LR. 2016. Autophagy-mediated longevity is modulated by lipoprotein biogenesis. *Autophagy* **12**:261–272.
- Shi C, Murphy CT. 2014. Mating induces shrinking and death in *Caenorhabditis* mothers. *Science* **343**:536–540.
- Shi C, Rannels AM, Murphy CT. 2017. Mating and male pheromone kill *Caenorhabditis* males through distinct mechanisms. *eLife* **6**:e23493.
- Srinivasan J, Kaplan F, Ajredini R, Zachariah C, Alborn HT, Teal PE, Malik RU, Edison AS, Sternberg PW, Schroeder FC. 2008. A blend of small molecules regulates both mating and development in *Caenorhabditis elegans*. *Nature* **454**:1115–1118.
- Srinivasan J, von Reuss SH, Bose N, Zaslaver A, Mahanti P, Ho MC, O'Doherty OG, Edison AS, Sternberg PW, Schroeder FC. 2012. A modular library of small molecule signals regulates social behaviors in *Caenorhabditis elegans*. *PLoS Biol.* **10**:e1001237.
- Taylor SR, Santpere G, Weinreb A, Barrett A, Reilly MB, Xu C, Varol E, Oikonomou P, Glenwinkel L, McWhirter R, et al. 2021. Molecular topography of an entire nervous system. *Cell* **184**:4329–4347.e23.
- Teuscher AC, Ewald CY. 2018. Overcoming autofluorescence to assess GFP expression during normal physiology and aging in *Caenorhabditis elegans*. *Bio Protoc.* **8**:e2940.
- Ting JJ, Woodruff GC, Leung G, Shin NR, Cutter AD, Haag ES. 2014. Intense sperm-mediated sexual conflict promotes reproductive isolation in *Caenorhabditis* nematodes. *PLoS Biol.* **12**:e1001915.
- van Rossum G, Drake FL. 2009. *Python 3 reference manual*. Scotts Valley (CA): CreateSpace.
- Wolf FA, Angerer P, Theis FJ. 2018. SCANPY: large-scale single-cell gene expression data analysis. *Genome Biol.* **19**:15.
- Wolf FA, Hamey FK, Plass M, Solana J, Dahlin JS, Gottgens B, Rajewsky N, Simon L, Theis FJ. 2019. PAGA: graph abstraction reconciles clustering with trajectory inference through a topology preserving map of single cells. *Genome Biol.* **20**:59.
- Wu D, Wang Z, Huang J, Huang L, Zhang S, Zhao R, Li W, Chen D, Ou G. 2022. An antagonistic pleiotropic gene regulates the reproduction and longevity tradeoff. *Proc Natl Acad Sci U S A.* **119**:e2120311119.
- Wyatt TD. 2014. *Pheromones and animal behavior: chemical signals and signatures*. Cambridge: Cambridge University Press.
- Zhao Y, Gilliat AF, Ziehm M, Turmaine M, Wang H, Ezcurra M, Yang C, Phillips G, McBay D, Zhang WB, et al. 2017. Two forms of death in ageing *Caenorhabditis elegans*. *Nat Commun.* **8**:15458.
- Zimmerman SM, Hinkson IV, Elias JE, Kim SK. 2015. Reproductive aging drives protein accumulation in the uterus and limits lifespan in *C. elegans*. *PLoS Genet.* **11**:e1005725.